

U. S. DEPARTMENT OF COMMERCE  
NATIONAL OCEANIC AND ATMOSPHERIC ADMINISTRATION  
NATIONAL WEATHER SERVICE  
NATIONAL METEOROLOGICAL CENTER

OFFICE NOTE 178

The NMC 9-Layer Global Primitive Equation  
Model on a Latitude-Longitude Grid

John D. Stackpole  
Development Division

MAY 1978

This is an unreviewed manuscript, primarily  
intended for informal exchange of information  
among NMC staff members.

# THE NMC 9-LAYER GLOBAL PRIMITIVE EQUATION MODEL

## ON A LATITUDE-LONGITUDE GRID

(National Meteorological Center, NOAA, USA)

### Introduction

In November 1972, the National Meteorological Center (NMC) put into operation a fully global analysis-forecast system employing a Hough function spectral analysis and an 8-layer primitive equation forecast model on a  $5^{\circ}$  latitude-longitude grid. The analysis forecast set was run twice per day with the 12-hour forecast serving as the first guess for the analysis at the next observation time. The forecast model was described in GARP Publications Series No. 14.

Since that time a number of evolutionary changes have taken place in both the analysis system and the forecast model. The principal changes in the model have been a) changing from 8 to 9 forecast layers (and eliminating the constant potential temperature "thetasphere" layer at the top); b) eliminating the "boundary layer", so that there are now 6 equal pressure layers in the troposphere, and three in the stratosphere; c) changing the resolution from a  $5^{\circ}$  to a  $2.5^{\circ}$  longitude-latitude grid; and d) alterations to the finite difference calculations of the hydrostatic equation, large scale precipitation modeling and convective precipitation modeling. The principal changes in the analysis system are: a) a change from a 12 hour forecast/analysis update cycle to a 6 hour cycle, thus taking better account of asynoptic data (e.g. satellite observations); and b) a change in the analysis method from the Hough spectral technique to an Optimum Interpolation analysis system, still on a 6 hour update cycle.

---

This model description has been prepared by J. D. Stackpole.

What follows is a description of the physics and numerics of the forecast model. For a description of the Hough function analysis method, the reader is referred to Flattery (1971), and, for a description of the Optimum Interpolation analysis method, to The Proceedings of the 3rd AMS NWP Conference, April 1977, Omaha.

### Basic Equations

For the convenience of the reader, the hydrostatic meteorological equations in spherical coordinates and an arbitrary vertical coordinate  $\sigma$  are here transcribed:

$$\frac{\partial u}{\partial t} + \dot{\sigma} \frac{\partial u}{\partial \sigma} + u \frac{\partial u}{\partial x} + v \frac{\partial u}{\partial y} - \frac{uv}{r} \tan \phi - fv + g \frac{\partial Z}{\partial x} + c_p \theta \frac{\partial \pi}{\partial x} + F_x = 0 \quad (1)$$

$$\frac{\partial v}{\partial t} + \dot{\sigma} \frac{\partial v}{\partial \sigma} + u \frac{\partial v}{\partial x} + v \frac{\partial v}{\partial y} + \frac{vu}{r} \tan \phi + fu + g \frac{\partial Z}{\partial y} + c_p \theta \frac{\partial \pi}{\partial y} + F_y = 0 \quad (2)$$

$$g \frac{\partial Z}{\partial \sigma} + c_p \theta \frac{\partial \pi}{\partial \sigma} = 0 \quad (3)$$

$$\frac{\partial \theta}{\partial t} + \dot{\sigma} \frac{\partial \theta}{\partial \sigma} + u \frac{\partial \theta}{\partial x} + v \frac{\partial \theta}{\partial y} + H = 0 \quad (4)$$

$$\frac{\partial p_\sigma}{\partial t} + \frac{\partial}{\partial \sigma} (\dot{\sigma} p_\sigma) + \frac{\partial}{\partial x} (u p_\sigma) + \frac{\partial}{\partial y} (v p_\sigma) - \frac{p_\sigma v}{r} \tan \phi = 0 \quad (5)$$

$$\frac{\partial q}{\partial t} + \dot{\sigma} \frac{\partial q}{\partial \sigma} + u \frac{\partial q}{\partial x} + v \frac{\partial q}{\partial y} + EP = 0 \quad (6)$$

$$\pi = (p/1000)^{R/c_p} \quad (p \text{ in mb}) \quad (7)$$

Most of the symbols have their usual meaning; in spherical coordinates where  $\lambda$  is longitude,  $\phi$  latitude and  $r$  the radius of the (spherical) earth

$$\begin{aligned} u &= r \cos\phi \frac{d\lambda}{dt} & v &= r \frac{d\phi}{dt} \\ \frac{\partial}{\partial x} &= \frac{\partial}{r \cos\phi \partial \lambda} & \frac{\partial}{\partial y} &= \frac{\partial}{r \partial \phi} \end{aligned}$$

and the less familiar terms are

$\sigma = \frac{d\sigma}{dt}$  the vertical velocity;

$F_x, F_y$  = the x and y direction frictional terms;

H in Eq. (4) stands for various diabatic heating and cooling terms detailed below;

$p_{\sigma}$  in Eq. (5) is  $\partial p / \partial \sigma$ ;

EP in Eq. (6) stands for evaporation and precipitation processes which alter  $q$ , the specific humidity;

$\pi$ , the Exner function, is defined by Eq. (7).

An eighth equation is needed to close the set--it serves to define the vertical coordinate; we use the Phillips (1957)  $\sigma$  system as modified by Shumand and Hovermale (1968). Given two quasi-horizontal surfaces of known pressure  $p_U$  for the upper one,  $p_L$  for the lower,

$$\sigma = \frac{p - p_U}{p_L - p_U} \quad (8)$$

A region of the model atmosphere between a given pair of  $p_U, p_L$  surfaces is called a  $\sigma$  domain, levels or layers specified by particular  $\sigma$  values within a single domain are called (naturally)  $\sigma$  levels (or surfaces) and  $\sigma$  layers.

# Vertical Structure

Fig. 1 is a schematic diagram of the vertical structure of the 9-layer model with indications of the approximate pressures for the various  $\sigma$  surfaces.

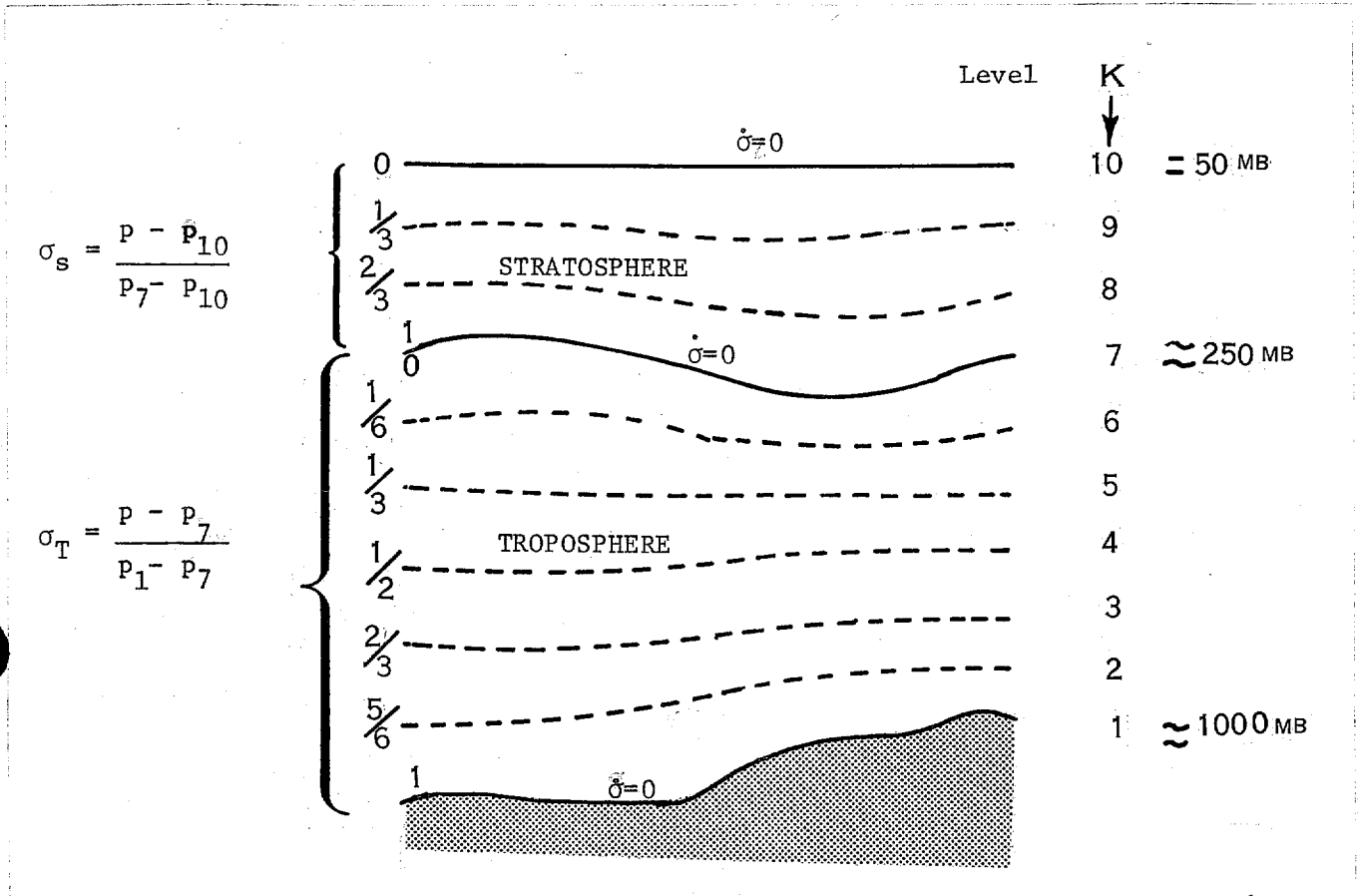


Fig. 1 Schematic Diagram of the vertical structure

Two  $\sigma$  domains are defined: a tropospheric and a stratospheric domain. The tropospheric domain is defined between the surface pressure,  $p_1$ , and the tropopause  $p_7$ :

$$\sigma_T = \frac{p - p_7}{p_1 - p_7}$$

The troposphere is divided into six layers of equal  $\sigma$  (or pressure) thickness. The stratosphere extends from the tropopause to a constant (in space and time) pressure surface at 50 mb ( $p_{10}$ ):

$$\sigma_S = \frac{p - p_{10}}{p_7 - p_{10}},$$

and is divided into three equal  $p$  (or  $\sigma$ ) layers.

Boundary conditions are stated in terms of  $\sigma$  and the assertion that  $p_{10} = 50$  mb for all time and space. For  $k$  levels 1, 7, and 10  $\sigma = 0$ , i.e., there is no transport of anything (mass, momentum, whatever) in or out of either sigma-domain from "outside" or from the other domain. The latter condition assures the integrity of the model tropopause at  $p_7$ . Indeed this condition effectively defines the model "tropopause" as a material surface between the stratosphere and troposphere.

The forecast variables,  $u$ ,  $v$ , and  $\theta$ , are carried as averages or representative values within each  $\sigma$  layer,  $p_0$  is forecast for the two domains, and  $q$  is carried in the five lowest layers.

### Horizontal Structure

The horizontal structure is quite straightforward: the data are carried on a regular 2.5 longitude latitude grid (with no elimination of points or other artificial devices near the poles). At the poles, all of the latitude-longitude intersection points refer to the same geographic point, hence the scalar variables  $\theta$ ,  $p_0$ ,  $q$  and others derived from them ( $\pi$ ,  $Z$ , etc.) will be the same at all the pole points, while the one vector wind at the pole is resolved into the  $u$  and  $v$  components appropriate to the meridian along which one would approach the pole.

### Finite-Difference Formulation

We shall employ the notation introduced by Shuman (1962), to wit: for any quantity  $f$  located at equally spaced points  $f_i$ , longitudinal differencing is

$$f_x = \frac{f_{i+\frac{1}{2}} - f_{i-\frac{1}{2}}}{\Delta x}; \Delta x = r \cos \phi \Delta \lambda$$

and averaging is

$$\overline{f^x} = 0.5(f_{i+\frac{1}{2}} + f_{i-\frac{1}{2}})$$

with analogous expressions for the latitudinal and vertical terms.

Employing this notation, we can write the tendency equations in finite differences as

$$\begin{aligned} \frac{\partial u}{\partial t} + \overline{\dot{\sigma}_{NS}^x u \sigma} + \overline{\dot{\sigma}_{EW}^y u \sigma} + \overline{u^x u_x} + \overline{v^y u_y} \\ - \frac{\overline{uv}^x}{r} \tan \phi - \frac{\overline{v^x}}{v} f + g Z_x + c_p \overline{\theta^x} \frac{\pi_x^{bp}}{\pi_x} + F_x = 0 \end{aligned} \quad (9)$$

$$\begin{aligned} \frac{\partial v}{\partial t} + \overline{\dot{\sigma}_{NS}^x v \sigma} + \overline{\dot{\sigma}_{EW}^y v \sigma} + \overline{u^x v_x} + \overline{v^y v_y} \\ + \frac{\overline{uv}^y}{r} \tan \phi + \frac{\overline{u^y}}{u} f + g Z_y + c_p \overline{\theta^y} \frac{\pi_y^{bp}}{\pi_y} + F_y = 0 \end{aligned} \quad (10)$$

$$\frac{\partial \theta}{\partial t} + \dot{\sigma}_{NS} \frac{-x}{\sigma} + \dot{\sigma}_{EW} \frac{-y}{\sigma} + \frac{-x}{\sigma} \frac{y}{\sigma} + \frac{-y}{\sigma} \frac{x}{\sigma} + H = 0 \quad (11)$$

$$\begin{aligned} \frac{\partial p_{\sigma}}{\partial t} + \dot{\sigma}_{NS} \frac{-x}{\sigma} p_{\sigma} + \dot{\sigma}_{EW} \frac{-y}{\sigma} p_{\sigma} + \frac{-x}{\sigma} p_{\sigma x} + \frac{-y}{\sigma} p_{\sigma y} \\ + \frac{-x}{\sigma} p_{\sigma} + \frac{-y}{\sigma} p_{\sigma} - \frac{p_{\sigma} v}{r} \tan \phi = 0 \end{aligned} \quad (12)$$

$$\frac{\partial q}{\partial t} + \dot{\sigma}_{NS} \frac{-x}{\sigma} q_{\sigma} + \dot{\sigma}_{EW} \frac{-y}{\sigma} q_{\sigma} + \frac{-x}{\sigma} q_x + \frac{-y}{\sigma} q_y + EP = 0 \quad (13)$$

The expressions for  $\pi$  and  $\sigma$  remain as originally written.

The finite difference hydrostatic equation receives special treatment. Following the discussions by Brown (1974) and Phillips (1974) the geopotential is constructed to be defined in the middle of each  $\sigma$ -layer (the absence of any vertical averaging operator on the  $Z_x$  and  $Z_y$  terms of equations 9 and 10 indicates this) and the value of the exner function that, in effect, defines the "middle" of the layer ( $\pi^{bp}$  in Eqns. 9 and 10) is defined in terms of the  $\pi$  and  $p$  values at the adjacent levels. In more detail, the computational sequence is: given values of  $p_{\sigma}$  for the two domains (forecast from Eqn. (12)), the values of pressure and  $\pi$  at each  $\sigma$ -surface are found by straightforward applications of the definitions of  $\sigma$  and  $\pi$ , Eqns. 8 and 7. The value of  $\pi$  for the  $k^{th}$  layer (the  $k^{th}$  layer is the one just above the  $k^{th}$  level) is given by

$$\pi_k^{bp} = \frac{\pi_k p_k - \pi_{k+1} p_{k+1}}{(1+\chi)(p_k - p_{k+1})} \quad \chi = R/C_p \quad (14)$$

i.e. the pressure weighted mean of the  $\sigma$ -surface  $\pi$  values.



The computational form of the hydrostatic equation is dictated by requirements of conservation of total energy in the finite difference equations - these are the results of the Brown and Phillips studies. We start with the known height of the terrain  $Z^*$ . The distance from the ground to the middle of the first layer is given by

$$Z_1 - Z^* = \frac{C_p}{g} \left\{ \sum_{k=1}^6 \Theta_k \left[ \sigma_{T_{k+1}} \left( \pi_k^{bp} - \pi_{k+1} \right) - \sigma_{T_k} \left( \pi_k^{bp} - \pi_k \right) \right] + \sum_{k=2}^6 \frac{1}{2} \left( \Theta_k + \Theta_{k-1} \right) \left( \pi_k^{bp} - \pi_{k-1}^{bp} \right) \sigma_{T_k} \right\} \quad (15)$$

a rather messy combination of layer temperatures ( $\Theta_k$ ), layer exner functions ( $\pi_k^{bp}$ ) level exner function ( $\pi_k$ ), and  $\sigma$ -level values of troposphere domain sigma ( $\sigma_{T_k}$ ), summed over the troposphere. The remaining mid-layer values of  $Z$  for the troposphere are much more straightforward:

$$Z_k = Z_{k-1} - \frac{C_p}{g} \left\{ \frac{1}{2} \left( \Theta_k + \Theta_{k-1} \right) \left( \pi_{k-1}^{bp} - \pi_k^{bp} \right) \right\} \quad (16)$$

i.e. the thickness between layers is a simple finite difference analogue of Eqn. 3.

The "hydrostatic jump" from layer 6 to layer 7 (across the model tropopause) again gets complicated. We end up with:

$$Z_7 - Z_6 = - \left( Z_1 - Z^* \right) + \frac{C_p}{g} \left\{ \sum_{k=1}^6 \Theta_k \left[ \left( \pi_k^{bp} - \pi_{k+1} \right) - \left( \pi_k^{bp} - \pi_k \right) \right] + \sum_{k=7}^9 \Theta_k \left[ \sigma_{S_{k+1}} \left( \pi_k^{bp} - \pi_{k+1} \right) - \sigma_{S_k} \left( \pi_k^{bp} - \pi_k \right) \right] + \sum_{k=2}^6 \frac{1}{2} \left( \Theta_k + \Theta_{k-1} \right) \left( \pi_k^{bp} - \pi_{k-1}^{bp} \right) \sigma_{T_k} + \sum_{k=8}^9 \frac{1}{2} \left( \Theta_k + \Theta_{k-1} \right) \left( \pi_k^{bp} - \pi_{k-1}^{bp} \right) \sigma_{S_k} \right\} \quad (17)$$

combining both tropospheric and stratospheric quantities. The remaining stratospheric layer values are obtained from Eqn. 16.

These expressions compute the tendencies in the  $\lambda$ - $\phi$  boxes--the necessary task of returning the forecast information back to the grid points is sufficiently complicated to merit discussion in a separate section.

The motivation for selecting the particular finite difference system found here rested mainly on eliminating numerical problems relating to the poles of the longitude latitude grid without introducing excessively unreasonable devices at the poles. The near-pole computations are somewhat special of course. Once the tendencies are computed in all the boxes, the ones in the pie-shaped "boxes" adjacent to the poles get special treatment. If  $u'_{ti}$  and  $v'_{ti}$  are those tendencies, a single vector tendency is computed by averaging all around the pole

$$\begin{aligned} U_t &= \frac{1}{N} \sum_{i=1}^N u'_{ti} \cos \lambda_i - v'_{ti} \sin \lambda_i \\ V_t &= \frac{1}{N} \sum_{i=1}^N u'_{ti} \sin \lambda_i + v'_{ti} \cos \lambda_i \end{aligned} \quad (18)$$

(N is the number of boxes involved); the scalar quantity tendencies are also averaged all around the pole.

Then the original box tendencies are replaced by these average tendencies

$$\left. \begin{aligned} u_{ti} &= U_t \cos \lambda_i + V_t \sin \lambda_i \\ v_{ti} &= -U_t \sin \lambda_i + V_t \cos \lambda_i \end{aligned} \right\} \quad (19)$$

and

$$\theta_{ti} = \frac{1}{N} \sum_{k=1}^N \theta'_{tk}$$

for example; thus all the tendencies in the polar boxes are either equal, for the scalars, or are components of a single vector wind tendency.

The polar winds are not actually forecast--the prime meridian components are specified as the average of the previously forecast winds on the row south (or north) of the pole

$$\begin{aligned} U &= \frac{1}{N} \sum_{i=1}^N u_i \cos \lambda_i - v_i \sin \lambda_i \\ V &= \frac{1}{N} \sum_{i=1}^N u_i \sin \lambda_i + v_i \cos \lambda_i \end{aligned} \quad (20)$$

and the components are computed exactly as the averaged tendencies as in Eq. (19).

These polar devices, in conjunction with the form of the finite-difference equations, completely resolve and eliminate all the mathematical difficulties usually associated with the pole: infinite tangents, indefinite forms, etc.

#### Computation of the Vertical Velocity, $\dot{\sigma}$

The computation of  $\dot{\sigma}$  is easily described from the continuity equation (5). In the troposphere we first solve the continuity equation integrated (actually summed over the layers) over the entire domain (something we have to do anyway) for the  $p_\sigma$  tendency calculation. This takes the form

$$\frac{\partial p_{\sigma T}}{\partial t} = - \frac{1}{6} \sum_{k=1}^6 \left\{ u_k p_{\sigma x} + v_k p_{\sigma y} + (\bar{u}_{kx} + v_{ky}) p_\sigma - v_k p_\sigma \frac{\tan \phi}{r} \right\} \quad (21)$$

Here the  $k$  subscripts refer to the layers (there is no ambiguity between quantities defined at  $\sigma$ -levels, such as  $p$  and  $\pi$ , and layer defined quantities) and the  $x$  and  $y$  subscripts are derivatives (or finite differences). A similar expression applies to the stratosphere where the summation is over the three layers  $k=7, 8$  and  $9$ .

Once the  $p_\sigma$  tendency for the entire domain is obtained from Eq.(21), the continuity equations for each separate layer of the domain may be solved for  $\dot{\sigma}_\sigma$  in each layer. Given then that  $\dot{\sigma}=0$  at  $k$  levels 1, 7, and 10, the  $\dot{\sigma}$ 's for each level may be obtained straightforwardly in sequence.

When the horizontal differencing is reintroduced an additional complication arises in the form of a duplex  $\dot{\sigma}$  in Eqn. 12. The reader will note the presence of a  $\dot{\sigma}_{NS}$  and  $\dot{\sigma}_{EW}$ . These two  $\dot{\sigma}$  s represent the contribution to the total  $\dot{\sigma}$  by terms defined to exist along the northern and southern edges of the longitude-latitude boxes (those sharing a  $(\ )^{-x}$  or  $(\ )_x$  operation) and those lying on the east and west edges of the boxes (those sharing a  $(\ )^{-y}$  or  $(\ )_y$  operation) respectively. The entire  $\dot{\sigma}$  calculation procedure is done, in effect, twice; once where  $(\ )^{-x}$  and  $(\ )_x$  terms are used to form a partial  $p_\sigma$  tendency which is in turn used to compute  $\dot{\sigma}_{EW\sigma}$ , and then a second time using  $(\ )^{-y}$  and  $(\ )_y$  terms exclusively. This introduction of a duplex  $\dot{\sigma}$  is necessary to maintain the integrity of the finite difference system near the pole.

### Averaging Tendencies to Grid Points and Time Stepping

In order to eliminate the possibilities of linear instability introduced by the poleward convergence of the meridians, the tendency terms in the boxes undergo a horizontal averaging or smoothing (or convolution to use a more mathematical term). This is designed to have the effects of suppressing very short waves in the grid and bringing the tendency information from the grid boxes to the meridians where the grid points are located. Obviously the convolution or smoothing operator should expand in an east west direction, in terms of the number of tendency points included in it, such that it remains at a fixed length with respect to the earth. But further specifications of the operator: its shape, equatorial width, etc., are not self evident.

Some numerical experimentation and heuristic argument (Stackpole, 1972) suggested that a triangular shaped operator was appropriate. The apex of the triangle would be placed on the meridian of the grid point to which the tendencies were to be averaged and the tendency values at a distance of  $\frac{1}{2}$  grid interval,  $1\frac{1}{2}$  intervals,  $2\frac{1}{2}$  intervals, etc. would be combined.

The (unnormalized) weights for such a function would be

$$w = \begin{cases} 1. - \frac{\chi}{L \sec \phi_0} & \chi = 0.5, 1.5, 2.5, \dots < L \sec \phi_0 \\ 0. & \chi \geq L \sec \phi_0 \end{cases}$$

The longitudinal expansion of the triangle is accomplished by the  $\sec \phi_0$  term ( $\phi_0$  is the latitude of the center of the row of tendency point boxes) and  $\chi$  is specified in grid length units. The  $L$  term is pure engineering - its specification determines the equatorial width of the triangle ( $L$  is

one half the base of the triangle): Too small a value would result in not enough smoothing and instabilities could develop; too large a value would include more points than strictly necessary into a rather expensive computation. Experimentally  $L=1.5$  worked well.

A portion of ~~the~~ argument that led to the choice of a triangular shaped function (and away from a simple rectangular shaped "running mean" function) was consideration of the Fourier Transform of the function. The transform of the triangle, viewed as a spectral response function, has no negative values (while the transform of the rectangle does) and this appears, heuristically, to be a good thing. Fourier transform theory applies to continuous variables; Shuman and Shuman (1975) undertook studies of smoothing of discrete variables. Some implications from their work are that a strictly triangular weight does have a negative response function at some frequencies in the discrete data case, but a linear combination of two triangles, one of them 2 grid intervals wider than the other, does not. In practice this boils down to the extreme points included in the triangular function being given a slightly larger weight than they would get were an exact triangular weighting used. The proper width of the weighting triangle can be arrived at theoretically with arguments based on satisfying the CFL linear stability criteria. It turns out that width is very close to the width arrived at experimentally ( $L=1.5$ ) earlier.

Once the tendency values have been averaged to the meridians of the longitude latitude grid a simple two point north-south averaging along meridians returns the tendencies to the grid points. This latter averaging does not change with latitude. The wind tendencies are appropriately rotated during the averaging: If the rotation is assumed to take place on

a locally tangent cone, tangent at the point to which the averaging goes, with coordinates  $(\lambda_0, \phi_0)$ , the angle of rotation is

$$\alpha = (\lambda_0 - \lambda) \sin \phi_0$$

and the local wind tendency components  $U_t, V_t$  are expressed as

$$\begin{aligned} U_t &= u_t \cos \alpha + v_t \sin \alpha \\ V_t &= -u_t \sin \alpha + v_t \cos \alpha \end{aligned}$$

prior to the averaging.

Once the tendencies are returned to the gridpoints, the time extrapolation is performed using the conventional leapfrog method, e.g.,  $\partial \theta / \partial t \approx \frac{\theta_t - \theta_{t-1}}{\Delta t}$ , except at the initial step where a forward step is used.

With the forecast at the  $\tau+1$  time level available, along with the fields at  $\tau$  and  $\tau-1$ , a time averaging is performed, replacing the  $\tau$  fields by

$$\theta^{*\tau} = \theta^\tau + \frac{\alpha}{2} (\theta^{\tau+1} - 2\theta^\tau + \theta^{*\tau-1})$$

Experimentally  $\alpha = 0.5$  is an appropriate value. This time smoother was first suggested by Robert (1966), and has been analyzed by Gerrity and Scolnik (1971) and Asselin (1972). A time step of 10 minutes is entirely satisfactory on the  $2.5^\circ$  grid currently in use.

### Initial Data

The initial conditions for the forecast model can come from two sources. The primary source, in the routine analysis and forecast cycle, is the optimum interpolation analysis. In that the results of this analysis are entirely within  $\sigma$ -coordinates and on the  $2.5^\circ$  grid nothing additional needs to be done. The model merely swallows up the O/I analysis and proceeds to forecast from it.

In those cases where an O/I analysis is not available (re-runs of pre-O/I implementation cases, special tests, etc.) it is necessary to revert back to the Hough analysis. The end results of the Hough function analysis are heights, winds and temperatures on the 12 mandatory levels up to 50 mb plus surface temperature, tropopause pressure and relative humidity on the six mandatory levels up to and including 300 mb. These data are on the  $2.5^\circ$  grid over the entire globe (10875 points per field). Transferring this information to the nine sigma layers of the model is done in essentially the same manner as in the 6-layer model described by Shuman and Hovermale (1968). In outline the computational sequence for each grid point is:

a) Given the height of the ground, the two mandatory levels which bracket the ground surface (one above, one below) are found. If the 1000 mb height is above the ground, the 1000 mb and 850 mb mandatory level information are used. The known (analyzed) heights and temperatures at the mandatory levels and the known height of the ground constitute sufficient information to interpolate, using the hydrostatic equation,

$$g\Delta Z = -RT\Delta \ln p$$



for the pressure at the ground, provided some assumption is made about the variation of temperature with pressure. We assume that  $T$  varies linearly with  $\ln p$ . In such an assumption two pieces of information are needed: the lapse rate (slope) and the mean temperature of the layer. The slope is specified by the temperatures at the mandatory levels, the mean temperature is computed from the thickness of the mandatory layer and is assigned to a pressure given by the mean of the natural logarithms of the mandatory level pressures. Given, then, the pressure at the ground, a tropopause pressure analysis and the assertion that the topmost surface is at 50 mb, the  $\sigma$  coordinate system is completely defined. This then specifies the initial values of  $p_0$ , one of the parameters to be forecast.

b) The next step is to find the pairs of mandatory levels which bracket each of the  $\sigma$ -surfaces, with known pressures. Once found, the same hydrostatic interpolation as before is used, only this time we are finding the height at the known  $\sigma$ -surface pressures, rather than vice-versa. Once the heights are found the corresponding layer potential temperatures,  $\theta$ , are found, again hydrostatically:

$$\theta = - \frac{c_p}{g} \frac{\Delta z}{\Delta \pi},$$

and we, finally, have the initial values for the second of the five forecast parameters. Prior to their use the temperatures are checked for static stability and adjusted as necessary.

c) The initial winds are obtained in a more direct manner: they are merely interpolated to the middle of each  $\sigma$ -layer from the two mandatory levels which bracket the middle-layer value of pressure. The wind components are assumed to vary linearly with  $\ln p$  between the mandatory levels. No further adjustments to the winds are made - the Hough function winds are nondivergent on pressure surfaces and nearly so in the  $\sigma$  coordinates.

d) The initial values of the specific humidity are obtained by simple interpolations of the analyzed relative humidity to the middle of the lowest five layers from the bracketing mandatory levels, again assuming a linear variation with  $\ln p$ . The already available  $\sigma$ -layer values of  $\theta$  and  $p$  serve to specify the saturation specific humidity - multiplication by the relative humidity gives the required initial values. Prior to their use in the model the  $q$  values are scaled to conform to the quantitative precipitation forecast method - this will be detailed in a later section.

#### Assorted Physics Parameterizations

In addition to the basic hydrodynamics, the model includes a number of additional physical effects of varying degrees of sophistication. These are the effects that contribute to the  $F_x$ ,  $F_y$ ,  $H$ , and  $EP$  terms of Eqn. 1-6.

##### 1. Friction

The model senses the ground by incorporation of a frictional drag term--there is no other friction in the model, only a surface friction term. The expression is based on the Prandtl layer theory and takes the form

$$\left. \begin{aligned} F_x &= \frac{g\rho}{\Delta p} C_D |\vec{v}| u \\ F_y &= \frac{g\rho}{\Delta p} C_D |\vec{v}| v \end{aligned} \right\}$$

where  $\Delta p$  and  $\rho$  are the pressure thickness and mean density respectively of the lowest model layer.  $\underline{V}$  is the vector wind (with  $u$  and  $v$  the components of course) in that layer and  $C_D$  the drag coefficient. The drag coefficient varies with the nature of the terrain and an explanation of how it is evaluated can be found in Cressman (1960.) A set of longitude-latitude values of  $C_D$  have been constructed for the Southern Hemisphere.

Hydrostatically:

$$\rho = \frac{\Delta p}{c_p \theta \Delta \pi}$$

The winds,  $\Delta p$  and  $\Delta \pi$  are those of the lowest layer only and are taken from the  $\tau-1$  past time level, to avoid numerical instabilities.

## 2. Radiation

### A. Short-wave

The basic structure of the short-wave calculation follows the method of Manabe and Wetherald (1967) but with adaptations to allow for multilayer cloudiness and to render it more appropriate for a forecast model. The first of these latter adaptations is that water vapour absorption only is considered; the second is that diurnal variations of solar zenith angle are included.

The adaptations to include multilayer cloudiness can best be described in terms of the disposition of the downward and upward radiation streams. First, the fractional absorptivity of each layer is computed twice--once with the beam path length (precipitable water times cosecant of the solar zenith angle), secondly with the diffuse path length (precipitable water times 1.66, the Elsasser diffusion factor)--in both cases

using the Manabe-Wetherald absorption curves. Layers are either fully cloudy or clear--no partial cloudiness is modelled. Clouds are defined to exist if the relative humidity is 90 percent or greater in any layer.

A downward coursing stream of radiation then is partially absorbed in each layer according to the previously computed fractional absorptivities. The beam absorptivities are used until the radiation reaches a cloudy layer; for that layer then and any below it, the diffuse absorptivities are used. In addition, any cloudy layer will reflect a fraction of the radiation impinging upon it--this reflected upward diffuse radiation is also partially absorbed as it proceeds outward. The cloud albedo for the tropospheric layers from the ground up are 0.7, 0.6, 0.5, 0.4, and 0.3. The radiation reaching the ground is reflected with a geographically varying albedo and the resultant upward diffuse radiation is also partially absorbed on the way out, joining that radiation reflected from clouds. Further reflections from cloud bottoms are not considered. Couched in terms of the net flux at each level (positive direction downward), the resultant temperature change due to radiation is

$$\frac{\partial \theta}{\partial t} = - \frac{g}{c_p} \frac{\Delta F}{\Delta p}$$

#### B. Long-wave

For the computation of the fluxes of long-wave radiation, and consequent heating, we have elected to evaluate the integral for flux at a particular level in the atmosphere (measured in terms of the path length  $u$ ) as a function of frequency integrated black-body radiation and emissivity gradients, thus:

$$F(u) = \int_u^U B(u') \frac{\partial \epsilon(u, u')}{\partial u} du' + B(U) (1 - \epsilon(u, U)) \quad (22)$$

In this expression, the path length  $u$  serves double duty both as a coordinate and as a quantity involved in the physics.  $U$  is the limiting path length beyond which there are no sources of radiation, e.g., a cloudy layer, the ground or outer space.  $\epsilon(u, u')$  is the emissivity for the layer or layers from  $u$  to  $u'$  and is a function of the path length. Various expressions for emissivity have been used during development--none have appeared to be entirely satisfactory; at present we are using a linear approximation to the values derived by Kuhn (1963).

In the computations, the integral of Eq. (22) is replaced by layer-by-layer sums, beginning at each  $\sigma$  level of the model, summing downward for the upwelling radiation, upward for the downward radiative stream. When the temperature at a level is needed (a cloud base or top), it is obtained by interpolation from the adjacent layers. An exception: if we are at the point of computing the downward flux at the ground and the layer above the ground is cloudy, the black emission from that layer (all that would go into the ground-level down flux) is computed from the layer temperature rather than from some near-ground extrapolated temperature. Low stratus decks are not always foggy at the ground.

Once the long-wave fluxes are computed at all the relevant levels, Eq. (23) again serves to compute the resultant temperature changes.

All of the radiation calculations are computed from the  $\tau-1$  time level to avoid introducing numerical instabilities. These computations are done once per hour but the resultant temperature changes are used in each time step.

Moisture is forecast only in the 5 lowest layers of the model, which limits these radiative effects to the troposphere.

### 3. Surface Energy Exchanges

A still somewhat experimental effort at determining surface temperature over land and ice caps is incorporated via the assumption of no net flux of energy at the earth's surface. The previously computed values of net short-wave flux and downward long-wave flux are added to estimates of sensible and latent heat fluxes and "ground storage" terms, the balance is assumed to be in the form of long-wave flux up from the ground and from this latter is found the surface (radiative) temperature by solution of the Stephan-Boltzman equation. The sensible and latent energy fluxes also of course contribute to the change in temperature and specific humidity of the layer nearest to the ground.

The sensible heat flux is given by

$$H = \rho |\vec{V}| C_D C_p (\theta_1 - \theta^*) \quad (23)$$

where  $\theta_1$  is the temperature of the lowest layer and  $\theta^*$  that of the ground. If  $H$  is positive, a stable configuration, the flux is reduced by a factor of 10.

The latent heat flux is

$$LH = \rho |\vec{V}| C_D L (q_1 - w q_s^*) \quad (24)$$

$q_1$  is the specific humidity of the lowest layer;  $q_s^*$  the saturation specific humidity of the ground (a function of temperature and pressure only);  $w$  is the potential evaporation "wetness parameter" (Saltzman, 1967). Over water  $w=1$ , over land our first approximation is to set  $w$  equal to one minus the albedo, i.e., areas of high albedo tend to be relatively dry and conversely.

In the expressions for H and LH, the ground temperature and other variables used are those from the previous time step.

The ground flux term is treated differently. We avoid computing it explicitly by assuming that its effect will be to ameliorate changes in the surface temperature that would otherwise occur. The procedure is to compute the equilibrium temperature  $T_E$  in the absence of the ground effects, then form a temperature tendency for the surface temperature

$$\delta T = \beta (T_E - T^*) \quad (25)$$

and  $\beta (=0.05)$  specifies the amount of lag, "caused" by the "ground storage" in the surface temperature change. Over open water  $\beta=0$ , i.e., the sea surface temperature remains constant throughout the forecast. The surface temperature computation takes place at each time step.

A final note on the finite-difference configuration of this and the radiative computations of the previous section: all the calculations are made with  $(\ )^{xy}$  data, i.e., within each grid box. In this way, the tendencies will be consistent with the remainder of the equations and, perhaps more importantly, they share in the longitudinal averaging that eliminates linear instabilities.

A caveat: at the time of writing, the radiation calculations (including the surface energy terms and those portions of the precipitation modeling that bear upon the radiation computations) are undergoing rather close scrutiny. Some effects which were not given careful attention initially (e.g. radiative cooling of cloud tops, the effect of  $CO_2$ , partial cloud cover, the "ground storage") are undergoing refinement in a continuing effort to improve a not entirely adequate set of physical parameterizations.

#### 4. Precipitation and Latent Heat

Two forms of precipitation, with associated release of latent heat, can be generated by the model: large scale and convective. The "convective" rain is a sub-grid scale parameterization, the "large scale" rain is generated whenever the forecast values of specific humidity exceed various saturation thresholds in the layers. Both kinds of rain are generated from forecasts made within the longitude/latitude boxes, prior to the longitudinal averaging of the tendencies. This has the double advantage that the precipitation forecast is made on the finest resolution available, while the possibly substantial latent heat effects still undergo the longitudinal averaging needed to discourage linear instability - clearly the best of all possible worlds.

The large scale or saturation rain is dependent upon the forecast value of  $q$  and a forecast value of the saturation specific humidity  $q_s$ . The latter is a function of the forecast temperature and pressure in each layer. The  $q$  values are not compared directly against the  $q_s$  values but upon diminished values - the amount of diminution or scaling is a function of the  $\sigma$ -layer and temperature within the layer. Thus rain can fall ( $q$  greater than  $\hat{q}_s$  releases rain and latent heat -  $\hat{q}_s$  is the scaled saturation value) from a layer of less than 100% mean relative humidity. This is as it should be as the layers are quite thick relative to rain producing layers in the real atmosphere. The scaling factor,  $S_p$ , has the value 1.0 in the lowest layer (i.e. saturation in excess of a true 100% Relative humidity is required there for rain to fall), and a value of 0.8 (80% relative humidity for rain) in the top moist layer,  $\sigma$ -layer number 5. In the middle three layers the factor is the same (at any one grid point) but is a non-linear function of the lowest layer temperature,  $T$  ( $^{\circ}\text{C}$ ), according to these formulae



$$\begin{array}{ll}
 \left. \begin{array}{l} < -12.5^{\circ} \text{ C} \\ > -12.5^{\circ} \text{ C} \\ < 18.5^{\circ} \text{ C} \end{array} \right\} T & S_p = 0.8 \\
 & S_p = 0.8 - 0.005(0.015625 T^2 - 0.734375 T - 11.62109375) \\
 > 18.5^{\circ} \text{ C} & S_p = 0.9
 \end{array} \quad (26)$$

Obviously a system such as this contains a certain degree of empiricism - it represents a portion of a quadratic curve between the 0.8 and 0.9 limits located such that the flatter portion of the curve is at the higher temperature end. What we are stating here is that for rather cold lowest layer temperatures the saturation criteria, at higher layers in the model, is lower (80% relative humidity) than for rather warm lowest layer temperatures. Furthermore in the transition region there is a greater change in the saturation criterion (for a given change in lowest layer temperature) in colder air than in warmer air. These seemingly arbitrary adjustments to the saturation criteria serve to cause the model to generate rather satisfactory precipitation forecasts, particularly in the vicinity of fronts where the lowest layer temperature gradients are most pronounced.

Whenever  $q$  is forecast to exceed  $\hat{q}_s (=q_s \times S_p)$  condensation occurs in such an amount to bring  $q$  down to the  $\hat{q}_s$  value, (this is in the form of a contribution to the  $q$  tendency equation) and a corresponding amount of latent heat is released. Most of the latent heat serves to warm the layer in which the supersaturation/condensation occurs; however a fraction of the latent energy, given by a factor  $(6-k)/8$  where  $k$  is the number of the supersaturated layer, is placed in the lowest layer.

Finally, the rain does not fall undisturbed. Rain from a saturated layer falling into a relatively dry one will undergo partial evaporation and what's left will continue to the next layer, where the process may repeat.

The criteria for whether and how much evaporation takes place are similar, but not the same, as the saturation criteria. If the forecast relative humidity,  $q/q_s$ , is greater than 80% in the upper layers, or 82.5% in the lowest layer, no evaporation will take place. If  $q$  is less than  $0.8 q_s$  ( $0.825 q_s$  in layer 1) then the difference,  $0.8 q_s - q$ , is the moisture deficit for that layer. Finally then, a fraction,  $0.025 (6-k)^2$ , of the deficit for layer  $k$  will be eliminated by evaporation of falling rain, provided there is enough rain available, and the  $q$  tendency adjusted accordingly. If there is light rain falling into a low layer (small  $k$ ) with a large deficit, all the rain will evaporate, even though this may not fully make up the fractional deficit. When evaporation occurs, latent cooling takes place, again distributed in the vertical as the latent heating is.

One other source of moisture exists for the model atmosphere, evaporation from the ground. This is calculated in the section for the energy equilibrium at the surface outlined above - the latent heat flux either from the ground or to the ground, in the case of dew formation, is converted to flux of specific humidity and is a contribution to the  $q$  tendency equation for the lowest layer. The rate of evaporation is determined by the terms in the latent heat computation; however the flux is not allowed to continue if the lowest layer humidity reaches 80% or greater. This is analogous to the similar, but somewhat larger limitation on evaporation of falling rain. This 80% limitation is founded on some analysis of GATE observations of the oceanic boundary layer.

Because of these various scalings of the condensation process it would not be correct to use the initial analyses of  $q$  as they stand; they must be scaled to match. Once the initial  $\sigma$  layer  $q$  values are obtained they are multiplied by the appropriate values of  $S_p$ , Eqn. 26, with one exception. The lowest layer analyzed  $q$  is multiplied by 0.8 rather than 1.0 which is the value of  $S_p$  for that layer. This scaling assures that the values of  $q$  given to the model for forecasting are nowhere larger than  $\hat{q}_s$ , i.e. there is no initial supersaturation, and no initial latent heat shock.

The subgrid convective parameterization is, like many other such parameterizations, basically a series of tests of the instantaneous dynamic and thermodynamic conditions of the model. Then, depending upon whether the tests are satisfied, adjustments to the forecast quantities of the model, particularly  $u$ ,  $v$ ,  $q$ , and  $\theta$ , are made in amounts related to the quantitative results of the tests. The precise tests and numerical relationships are, of course, dependent upon the physical arguments and assumptions that went into the modeling of the subgrid phenomena. As with the large scale precipitation, all the various tests and calculations are computed within grid boxes, but, unlike the large scale, the adjustments to the tendency terms are made at the actual grid points around each "convective box" after the longitudinal and latitudinal averaging has been done. This enables us to model the motion of convective cloud groups relative to the mean wind in the box.

These are the tests which must be satisfied to, in effect, turn on cumulus convection in any one grid box:

- a) Grid box located between  $60^\circ\text{N}$  and  $60^\circ\text{S}$ .
- b) Upward motion at levels 2, 3 and 4 and motion increasing in magnitude with increasing elevation.

- c) Moist Static Energy ( $= C_p T + Lq + gZ$ ) must be decreasing through layers 1, 2, and 3.
- d) A near surface parcel, defined as a combination of surface and layer 1 temperature and humidity values, must be unstable with respect to the moist static energy at level 2, and must be above freezing.
- e) The ratio of the vertical velocity at level 2 to the maximum value observed in the column (the "fractional storm area coverage") must be between 0.005 and 0.95.
- f) The lifted condensation level for the near surface parcel must be below (higher pressure) level 3.

These conditions assure the presence of both large scale convergence through much of the troposphere, which provides a general lifting mechanism, and a deep layer of conditionally instable air which allows large cumuli to penetrate to the upper troposphere.

Given that the cumuli can exist within the box, the in-cloud conditions are specified as follows:

- a) The temperature and specific humidity are computed for each  $\sigma$  layer from a moist adiabat drawn from the lifted condensation level found in f) above.
- b) The wind is the vertical average of the large scale wind excluding the lowest layer.
- c) The in-cloud vertical velocity  $\dot{\sigma}_{ck}$  at level k is

$$\dot{\sigma}_{ck} = \frac{\dot{\sigma}_{\max}^2 - \dot{\sigma}_1 \dot{\sigma}_k}{\dot{\sigma}_{\max} - \dot{\sigma}_1}$$

up to the level of maximum vertical velocity,  $\dot{\sigma}_{\max}$ . From the  $\dot{\sigma}_{\max}$  level the vertical velocity decreases linearly to zero at the tropopause, level 7.

The tendency contributions from the cumuli are computed as additional vertical transport terms

$$\frac{\partial \psi}{\partial t} = - \frac{\partial}{\partial \sigma} \left[ \dot{\sigma}_c (\psi_c - \bar{\psi}) \right]$$

where  $\psi = \theta, q, u, v$ . The  $\psi_c$  are the in-cloud values and  $\bar{\psi}$  are the large scale box average values (the environment, if you will). The condensation in each layer, with associated latent heat, is

$$\dot{\sigma}_c \frac{\partial qc}{\partial \sigma}$$

Any condensation falls to the ground without any intermediate evaporation. These convective tendencies are computed for all layers above the one containing the lifted condensation level, excepting layer 6, the topmost tropospheric layer.

### Convective Adjustments

When a superadiabatic lapse rate develops, both the atmosphere and the numerical models become unstable. The atmosphere resolves the instability by mixing in the vertical all by itself, so to speak. We have to tell the model what to do and naturally we follow the atmosphere's lead and induce vertical mixing between the unstable layers.

The procedure is quite straightforward: If two dry layers are found to be unstable, they are both reassigned a mass weighted mean potential temperature

$$\theta_m = \frac{\theta_U \Delta p_U + \theta_L \Delta p_L}{\Delta p_U + \Delta p_L}$$

where U and L refer to the upper and lower layers respectively. The test then repeats for the next pair of layers above using the newly adjusted temperature in what is now the lower of the two layers.

### Presentation of Output

Almost all of the forecast maps from the model are presented on mandatory pressure levels which requires interpolations from the  $\sigma$  to the pressure coordinates. In general the interpolation methods are the same as for the initial p to  $\sigma$ : a hydrostatic calculation of Z on mandatory pressures given values of Z, T, and p at  $\sigma$  surfaces (where T varying linearly with  $\ln p$  is assumed in the integration of the hydrostatic equation), and simple linear (with  $\ln p$ ) interpolation of the other quantities u, v, T, q (or relative humidity) from the middle of the  $\sigma$  layers to the adjacent mandatory levels.

REFERENCES

- Asselin, R., 1972: "Frequency filter for time integrations." *Mon. Wea. Rev.*, 100, 487-490.
- Brown, J. A., 1974: "On vertical differencing in the  $\sigma$ -System." National Meteorological Center Office Note #92. U.S. National Weather Service.
- Cressman, G. P., 1960: "Improved terrain effects in barotropic forecasts." *Mon. Wea. Rev.*, 88, 327-342.
- Flattery, T. W., 1971: "Spectral models for global analysis and forecasting." Air Weather Service Technical Report 242, pp. 42-54.
- Gerrity, J. P. and Scolnik, S. H., 1971: "Further properties of time averaging as applied to wave type and damping type equations." Office Note #60, National Meteorological Center, NWS, Washington, D.C.
- Kuhn, P. M., 1963: "Radiometric observations of infrared flux emissivity of water vapor." *J. Appl. Meteor.*, 2, 368-378.
- Manabe, S. and Wetherald, R. T., 1967: "Thermal equilibrium of the atmosphere with a given distribution of relative humidity." *J. Atmos. Sci.*, 24, 241-259.
- Phillips, N. A., 1957: "A coordinate system having some special advantages for numerical forecasting." *J. Meteor.*, 14, 184-185.
- Phillips, N. A., 1974: "Application of Arakawa's energy conserving layer model to operational numerical weather prediction." National Meteorological Center Office Note #104. U.S. National Weather Service.

- Robert, A. J., 1966: "The integration of a low order spectral form of the primitive meteorological equations." *J. Met. Soc. Japan, Series 2*, 44, 237-245.
- Saltzman, B., 1967: "On the theory of the mean temperature of the earth's surface." *Tellus*, 19, 219-229.
- Shuman, F. G., 1962: "Numerical experiments with the primitive equations." Proceedings of the International Symposium on Numerical Weather Prediction, Tokyo, November 7-13, 1960, *J. Met. Soc. Japan*, 85-107.
- Shuman, F. G. and Hovermale, J. B., 1968: "An operational six-layer primitive equation forecast model." *J. Appl. Meteor.*, 7, 525-547.
- Shuman, F. G. and Shuman, F. G. D., 1975: "Theory of smoothing discrete functions." National Meteorological Center Office Note #111. U.S. National Weather Service.
- Stackpole, J. D., 1967: "Numerical analysis of atmospheric soundings." *J. Appl. Meteor.*, 6, 464-467.
- Stackpole, J. D., 1972: "On the longitudinal smoothing of the tendency fields in the 8-layer hemispheric PE model." National Meteorological Center Office Note #69. U.S. National Weather Service.